

# Conservation relations and anisotropic transmission resonances in one-dimensional $\mathcal{PT}$ -symmetric photonic heterostructures

Li Ge

*Department of Electrical Engineering, Princeton University, Princeton, New Jersey 08544, USA*

Y. D. Chong and A. D. Stone

*Department of Applied Physics, Yale University, New Haven, Connecticut 06520, USA*

(Received 21 December 2011; published 2 February 2012)

We analyze the optical properties of one-dimensional  $\mathcal{PT}$ -symmetric structures of arbitrary complexity. These structures violate normal unitarity (photon flux conservation) but are shown to satisfy generalized unitarity relations, which relate the elements of the scattering matrix and lead to a conservation relation in terms of the transmittance and (left and right) reflectances. One implication of this relation is that there exist anisotropic transmission resonances in  $\mathcal{PT}$ -symmetric systems, frequencies at which there is unit transmission and zero reflection, but only for waves incident from a single side. The spatial profile of these transmission resonances is symmetric, and they can occur even at  $\mathcal{PT}$ -symmetry-breaking points. The general conservation relations can be utilized as an experimental signature of the presence of  $\mathcal{PT}$  symmetry and of  $\mathcal{PT}$ -symmetry-breaking transitions. The uniqueness of  $\mathcal{PT}$ -symmetry-breaking transitions of the scattering matrix is briefly discussed by comparing to the corresponding non-Hermitian Hamiltonians.

DOI: [10.1103/PhysRevA.85.023802](https://doi.org/10.1103/PhysRevA.85.023802)

PACS number(s): 42.25.Bs, 42.25.Hz, 42.55.Ah

## I. INTRODUCTION

Motivated by fundamental studies of  $\mathcal{PT}$ -symmetric quantum Hamiltonians [1–3],  $\mathcal{PT}$ -symmetric photonic structures have attracted considerable interest in the past few years. These are structures with balanced gain and loss; in the case of a one-dimensional (1D) structure, this means that there is a symmetry point (chosen to be the origin,  $x = 0$ ) around which the linear index of refraction satisfies  $n^*(-x) = n(x)$ . Such structures were first studied in Refs. [4,5] and were shown to exhibit a variety of exotic photon transport phenomena, such as double refraction [5], power oscillations [5–7], and nonmonotonic behavior of the transmission loss with increased dissipation [8]. The initial studies focused on parallel waveguide structures with alternating loss and gain, in which the transverse variation of the electrical field, in the paraxial approximation to the wave equation, maps precisely onto a 1D or discrete Schrödinger equation, similar to the earlier quantum studies [4–9]. The parallel waveguide realization of  $\mathcal{PT}$ -symmetric photonic structures has recently found a promising application to compact optical isolators and circulators [10].

Recently, several authors have studied  $\mathcal{PT}$ -symmetric cavities and heterostructures [11–14], as well as general  $\mathcal{PT}$  scattering systems [13], using the full scalar wave equation, in the case that it obeys at least one  $\mathcal{PT}$ -symmetry operation. The current authors in particular emphasized the existence in such systems of  $\mathcal{PT}$ -symmetric and  $\mathcal{PT}$ -broken phases of the electromagnetic scattering matrix ( $S$  matrix). For the 1D case, the eigenvalues of the  $S$  matrix are unimodular in the  $\mathcal{PT}$ -symmetric phase, as they are in unitary systems, but photon flux is *not* conserved for most scattering processes, whereas in the  $\mathcal{PT}$ -broken phase, the  $S$ -matrix eigenvalues have reciprocal magnitudes, one greater than unity (corresponding to amplification) and the other less than unity (corresponding to attenuation). We and others [11–15] pointed out the existence of novel singular points in the broken-symmetry phase, which

we refer to as CPA laser points. At these points, one of the  $S$ -matrix eigenvalues goes to infinity (the usual lasing threshold condition), while the other goes to zero. The latter phenomenon corresponds to coherent perfect absorption (CPA) [16,17], in which a specific mode of the electromagnetic field, the time reversal of the lasing mode, is completely absorbed. For  $\mathcal{PT}$ -symmetric structures, these two phenomena must coincide [12,13]; i.e., at the laser threshold, in addition to a radiating mode of self-oscillation, there always exists an incident field pattern, which, instead of being amplified, is completely attenuated.

The rich behavior of 1D  $\mathcal{PT}$ -symmetric photonic structures violates the standard intuition that optical structures can be characterized by their single-pass gain or loss, which is always zero in these systems. The coincidence of both lasing and perfect absorption, and more generally the reciprocal amplification and attenuation displayed by the  $S$ -matrix eigenvalues, is a strict consequence of the symmetry property of the  $S$  matrix for such structures. In Ref. [13], this was expressed in arbitrary dimensions by the relation

$$(\mathcal{PT}) S(\omega^*) (\mathcal{PT}) = S^{-1}(\omega), \quad (1)$$

where  $\mathcal{P}$  is the parity operator (or indeed any discrete symmetry operator with  $\mathcal{P}^2 = 1$ ) and  $\mathcal{T}$  is the time-reversal operator (in the representation we will employ, this can be taken as the complex conjugation operator). By comparison, a  $\mathcal{T}$ -symmetric unitary  $S$  matrix would obey  $\mathcal{T} S(\omega^*) \mathcal{T} = S^{-1}(\omega)$ .

The set of  $S$  matrices obeying Eq. (1) can be shown to be isomorphic to a pseudounitary group, which in the 1D case is just  $U(1,1)$  [18]. In physical dimensions higher than one, there can be more than two input and output channels, and it is possible for the  $S$  matrix to be in a mixed “phase” with one subset of the eigenvalues forming “ $\mathcal{PT}$ -broken” amplifying or attenuating pairs and the remaining eigenvalues being “ $\mathcal{PT}$  symmetric” and flux conserving. For 1D structures, however,

there are only two eigenvalues, and they must either be both unimodular, or a nonunimodular inverse conjugate pair, except at the  $\mathcal{PT}$  transition point, an exceptional point at which the  $S$  matrix has only one eigenvector and eigenvalue [13].

Several specific cases of 1D  $\mathcal{PT}$ -symmetric structures have been studied [11–13,19], and in addition to the interesting CPA laser behavior, other intriguing properties have been found, such as unidirectional invisibility [19]. It is thus worthwhile to see which specific properties  $\mathcal{PT}$  symmetry imposes on transmission and reflection in arbitrary  $\mathcal{PT}$  structures, in both the symmetric and broken-symmetry phases. That is the goal of this work. In Sec. II, we show that 1D  $\mathcal{PT}$  structures obey certain strong conservation relations, which could be employed experimentally to determine if a given structure has realized  $\mathcal{PT}$  symmetry. In Sec. III, we examine a consequence of these conservation relations: the existence of transmission resonances in which the reflectance vanishes only for waves incident from one side of the structure, which we refer to as anisotropic transmission resonances (ATRs). The unidirectional invisibility phenomenon found by Lin *et al.* [19] is a special case of these ATRs. In Sec. IV, we derive a separate relation for the boundary between the  $\mathcal{PT}$ -symmetric and  $\mathcal{PT}$ -broken phases of the  $S$  matrix, involving the reflectance and transmittance for one-sided scattering processes. In Sec. V, we show that our conventional definition of the  $S$  matrix and its eigenvalues is physically meaningful, and in particular that its phase boundary can be related to  $\mathcal{PT}$ -breaking transitions in the spectrum of some  $\mathcal{PT}$ -symmetric Hamiltonian.

## II. GENERALIZED UNITARITY RELATIONS

We begin, following Longhi [12], with the 1D transfer matrix  $M$ , defined by (see Fig. 1)

$$\begin{pmatrix} A \\ B \end{pmatrix} = M \begin{pmatrix} C \\ D \end{pmatrix}. \quad (2)$$

For a  $\mathcal{PT}$ -symmetric heterostructure, the components of  $M$  obey the following properties [12]:

$$M_{22}(\omega) = M_{11}^*(\omega^*), \quad M_{12(21)}(\omega) = -M_{12(21)}^*(\omega^*), \quad (3)$$

where  $\omega$  is the frequency of the incident and scattered beams. For real  $\omega$ , these relations imply  $M_{22} = M_{11}^*$  and  $\text{Re}[M_{12}] = \text{Re}[M_{21}] = 0$ , which enables us to parametrize  $M$  as

$$M = \begin{pmatrix} a^* & ib \\ -ic & a \end{pmatrix}. \quad (4)$$

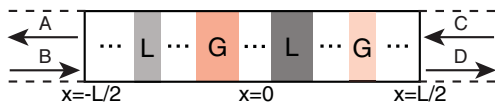


FIG. 1. (Color online) Schematic of a 1D  $\mathcal{PT}$ -symmetric photonic heterostructure, consisting of an arbitrary number of layers that are  $\mathcal{PT}$  symmetric about  $x = 0$ , i.e.,  $n(x) = n(-x)^*$ .  $G$  and  $L$  indicate gain and loss regions, and different color tones indicate different amplification or absorption strengths.

It is determined by three independent *real* quantities, i.e.,  $b$  and the phase and amplitude of  $a$ . The parameter  $c$  is related to  $|a|, b$  by

$$bc = |a^2| - 1, \quad (5)$$

which arises from the quite general condition  $\det(M) = 1$  [20]. The parametrization using  $a, b$  is valid except when  $M_{12} = 0$ ; in that case,  $|a| = 1$  and  $c$  replaces  $b$  as the third independent parameter.

In the following discussion, we assume nonvanishing  $M_{11}$  and  $M_{22}$ , which holds everywhere except at CPA laser points [21]. The  $S$  matrix is defined by

$$\begin{pmatrix} A \\ D \end{pmatrix} = S \begin{pmatrix} B \\ C \end{pmatrix} \equiv \begin{pmatrix} r_L & t \\ t & r_R \end{pmatrix} \begin{pmatrix} B \\ C \end{pmatrix}, \quad (6)$$

where  $r_L$  and  $r_R$  are the reflection coefficients for light incident from the left and right, respectively, while  $t$  is the transmission coefficient, which is independent of the direction of incidence. The parametrization (4) gives

$$S = \frac{1}{a} \begin{pmatrix} ib & 1 \\ 1 & ic \end{pmatrix}. \quad (7)$$

Thus, the reflection coefficients are  $r_L = ib/a$  and  $r_R = ic/a$ , which are unequal in magnitude but can differ in phase by only 0 or  $\pi$ , and the transmission coefficient is  $t = 1/a$ . Note that  $S$  satisfies the symmetry relation (1), with  $\mathcal{P} = \begin{pmatrix} 0 & 1 \\ 1 & 0 \end{pmatrix}$  and  $\mathcal{T}$  the complex conjugation operator. By using (5), we obtain the following exact “generalized unitarity relation”:

$$r_L r_R = t^2 \left( 1 - \frac{1}{T} \right). \quad (8)$$

This leads to the conservation relation

$$|T - 1| = \sqrt{R_L R_R}, \quad (9)$$

where  $R_{L \text{ or } R} \equiv |r_{L \text{ or } R}|^2$  are the two reflectances and  $T \equiv |t|^2$  is the transmittance. In addition, Eqs. (7) and (8) lead to phase relationships among the reflection and transmission coefficients

$$\begin{aligned} \phi_R &= \phi_L, & \text{if } T < 1 \\ \phi_R &= \phi_L + \pi, & \text{if } T > 1 \end{aligned} \quad (10)$$

$$\phi_{L,R} = \phi_t \pm \pi/2,$$

where  $\phi_{L,R}, \phi_t$  are the phases of the reflection and transmission coefficients.

Equations (8) and (9) are the central results of this work. They are valid for all 1D photonic heterostructures with  $\mathcal{PT}$  symmetry; two examples are shown in Fig. 2.

For  $T < 1$ , Eq. (9) becomes  $T + \sqrt{R_L R_R} = 1$ . This is an intriguing generalization of the more familiar conservation relation  $R + T = 1$ , which applies to unitary ( $\mathcal{T}$ -symmetric)  $S$  matrices for which the left and right reflectances are necessarily equal. In the  $\mathcal{PT}$ -symmetric case, the geometric mean of the two reflectances,  $\sqrt{R_L R_R}$ , replaces the single reflectance  $R$ . Therefore, when  $T < 1$ , the scattering of a single incident wave from one side of the structure is subunitary (some flux is lost) and the scattering from the other side is superunitary (some flux is gained). As an exception, there can be an accidental degeneracy at which  $R_L = R_R$ , in which case the scattering

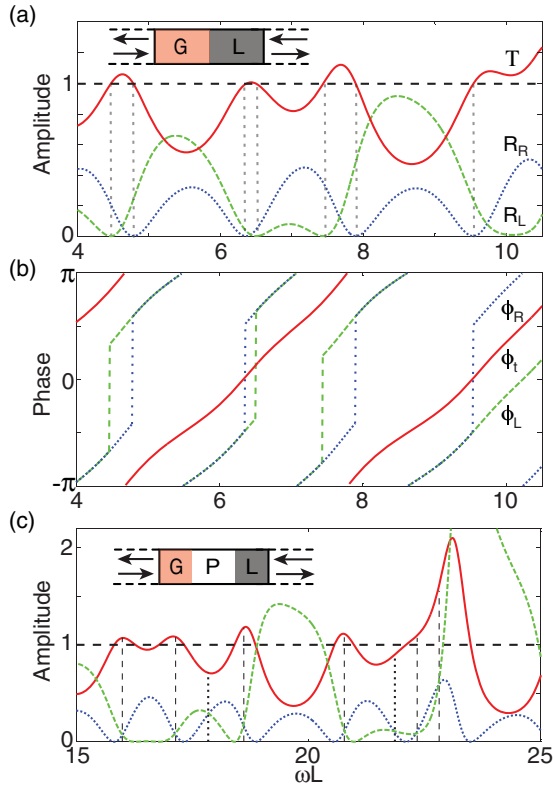


FIG. 2. (Color online) (a) Reflectance and transmittance of a 1D  $\mathcal{PT}$ -symmetric structure of index  $n = 2 \pm 0.2i$  and length  $L$ .  $R_L, R_R, T$  are labeled and indicated by the solid, dashed, and dotted curves, respectively. Zeros of the reflectances and the corresponding anisotropic transmission resonances ( $T = 1$ ) are marked by vertical dotted lines. The quantity  $R_L R_R + 2T - T^2 = 1$  is plotted as the horizontal dashed line to demonstrate the conservation relation (9). (b) Phases of  $r_L, r_R$ , and  $t$  in (a), demonstrating the reflection phase jumps at each ATR. (c) Same quantities are plotted as in (a), but the structure now has a passive region of length  $2L/5$  in the center. For this structure, we see that it is possible to have “accidental” flux-conserving points at which  $R_L = R_R (\equiv R \neq 0)$  and hence  $T + R = 1$ . Similarly, there are accidental pseudounitary points for which  $T - R = 1$ . They are indicated by vertical dotted and dashed lines, respectively. The speed of light in vacuum is taken to be unity and  $\omega L$  is dimensionless.

from both sides conserves flux. Such special cases do occur as a continuous parameter such as frequency is varied for nontrivial  $\mathcal{PT}$  systems ( $\text{Im}[n(x)] \neq 0$ ), as shown in Fig. 2(c).

For  $T > 1$ , all single-sided scattering processes are superunitary, and the conservation relation (9) can be rewritten as  $T - \sqrt{R_L R_R} = 1$ . Accidental reflectance degeneracies ( $R_L = R_R$ ) are also possible in this regime, giving the usual pseudounitary conservation relation  $T - R = 1$ , as shown in Fig. 2(c). All of these quantities actually diverge when approaching the CPA laser points, but they still satisfy the conservation relation (9).

Finally, we see that for  $T = 1$ , one of the reflectances must vanish (the other typically does not). Hence, the scattering for that direction of incidence is flux conserving, similar to resonant transmission in unitary structures. This phenomenon is analyzed in greater detail in Sec. III.

Interestingly, the  $S$  matrix describing three-wave mixing in the undepleted pump approximation corresponds to the special case where  $R_L = R_R$  [22,23]. The case  $T + R = 1$  describes frequency conversion by absorption or emission of a pump photon, and  $T - R = 1$  describes parametric amplification of both signal and idler by down conversion of pump photons. The relevance of a special case of  $\mathcal{PT}$  symmetry to optical parametric amplification and conversion has only very recently been appreciated.

An experimental concern in all  $\mathcal{PT}$  systems is how to confirm that one has truly realized a structure with  $\mathcal{PT}$  symmetry, i.e., that the gain and loss are balanced and the real index is symmetric. Equations (8)–(10) are strong constraints on the allowed scattering processes with a single incident beam for  $\mathcal{PT}$  systems, and can be used to test how close one is to the ideal symmetric structure.

### III. ANISOTROPIC FLUX-CONSERVING TRANSMISSION RESONANCES

As we have noted, Eq. (9) implies an interesting phenomenon: there exists a flux-conserving scattering process for incident waves on a single side if and only if  $T = 1$ , and one of  $R_L$  or  $R_R$  vanishes. We refer to such a process as an anisotropic transmission resonance (ATR). ATRs are different from the accidental flux-conserving processes that can occur for  $T < 1$ ; those, as we have seen, are accessible from either direction of incidence ( $R_L = R_R$ ). ATRs are a generalization of the flux-conserving transmission resonances of unitary systems, which are independent of the incidence direction. In Fig. 3, we show how two ATRs evolve out of a single transmission resonance of the unitary system as balanced gain and loss is added. Within the same structure, ATRs can occur for both left and right incidence, as the frequency is varied, but generally at different frequencies (to occur at the same frequency, a “doubly accidental” degeneracy  $R_L = R_R = 0$  would have to occur, requiring a second tuning parameter).

A surprising property of ATRs is that their intensity profile is spatially symmetric. This can be shown from the following analysis. If  $E(x)$  is the spatial profile of a left- (right-) going transmission resonance, then by a  $\mathcal{PT}$  operation  $E^*(-x)$  is also a left- (right-) going transmission resonance of the same structure. Since these two states happen at the same frequency, they must be identical (up to a phase  $\phi$ ) by the requirement of uniqueness:

$$E^*(-x) = e^{i\phi} E(x). \tag{11}$$

Hence, the intensity satisfies  $I(x) \equiv |E(x)|^2 = I(-x)$ . This result is consistent with the intuitive expectation that in order to conserve flux, the photons must on average spend equal amount of time in the loss and gain regions of the structure. Except at the ATRs, intensities do exhibit asymmetry for single-sided incidence, and in particular this is the case for a wave incident from the side with nonvanishing reflectance [see Figs. 3(e) and 3(f)].

Figure 3 shows two ATRs of a multilayer structure, one for each incidence direction, occurring at different frequencies. The frequencies are very similar because  $\text{Im}[n]$  is not very large and both ATRs arise from a bidirectional transmission resonance of the unitary ( $\text{Im}[n] = 0$ ) heterostructure. As

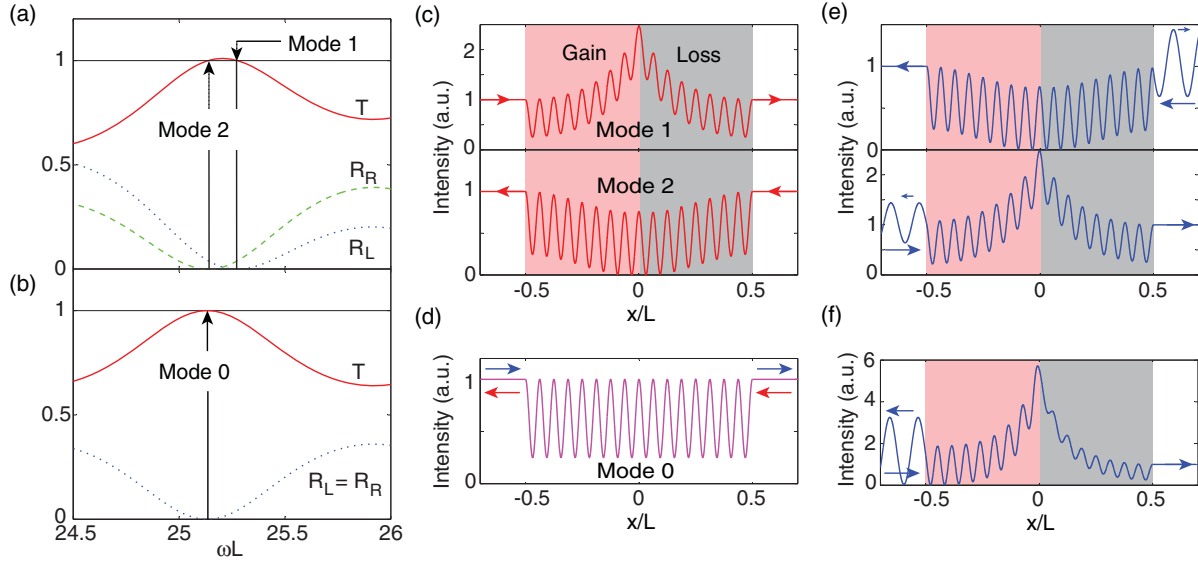


FIG. 3. (Color online) Asymmetric transmission resonances in a multilayer heterostructure. (a) Transmittance and reflectances as a function of frequency for  $\text{Im}[n] \neq 0$  and (b) for  $\text{Im}[n] = 0$ . Mode 0 is a bidirectional transmission resonance in the latter case. The structure has a constant  $\text{Re}[n] = 2$  and consists of 50 layers with  $\text{Im}[n]$  increasing (decreasing) stepwise from 0.004 ( $-0.004$ ) to 0.1 ( $-0.1$ ) toward the center in the loss (gain) half. The frequencies are  $\omega L = 25.275, 25.139$  in Modes 1 (wave incident from gain side) and 2 (wave incident from the loss side). Spatial profiles shown are (c) the ATRs, (d) unitary bidirectional transmission resonance, (e) “wrong” side scattering at the ATR frequencies, and (f) “wrong” side scattering at  $R_R = 0$  in the same structure, but with larger  $\text{Max}(\text{Im}[n]) = 0.17$ , showing a stronger asymmetry.

we add gain and loss to the unitary heterostructure, while preserving the  $\mathcal{PT}$  symmetry, the transmission resonances separate and their spatial profiles become more distinct. Figure 3(e) shows the asymmetric intensity profiles for waves incident at the ATR frequency, but from the “wrong” side (the side with nonvanishing reflectance). The asymmetry increases as the two ATRs move further apart with increasing gain or loss, as shown in Fig. 3(f).

Let us refer to the left and right halves of a  $\mathcal{PT}$ -symmetric heterostructure as  $U, V$ . We can write the reflection and transmission coefficients for the whole structure ( $r_L, r_R$ , and  $t$ ) in terms of the reflection and transmission coefficients for the  $U$  and  $V$  segments:

$$r_L = \frac{r_{L,U} - e^{i(\alpha_U + \alpha_V)} r_{L,U}^* r_{R,V}^*}{1 - e^{i(\alpha_U + \alpha_V)} r_{L,U}^* r_{R,V}^*}, \quad (12)$$

$$r_R = \frac{r_{R,V} - e^{i(\alpha_U + \alpha_V)} r_{R,V}^* r_{L,U}^*}{1 - e^{i(\alpha_U + \alpha_V)} r_{L,U}^* r_{R,V}^*}, \quad (13)$$

$$t = \frac{e^{i\alpha_U} (1 - r_{L,U}^* r_{R,V}^*)}{1 - e^{i(\alpha_U + \alpha_V)} r_{L,U}^* r_{R,V}^*}. \quad (14)$$

Here,  $\alpha_U$  or  $\alpha_V \equiv 2 \text{Arg}[t_U$  or  $V]$ . Note that if either  $r_{L,U} = 0$  or  $r_{R,V} = 0$  at some  $\omega$ , corresponding to a transmission resonance of  $U$  ( $V$ ) in the right (left) direction, the transmittance for the full structure will also be unity.

Thus, one type of ATR can arise from resonances of either half of the  $\mathcal{PT}$  system. This follows from  $\mathcal{PT}$  symmetry. First, using the time-reversal operation, a transmission resonance of  $S(nk)$  from the left must be a transmission resonance of  $S(n^*k)$  from the right (interchange gain and loss regions and interchange incoming and outgoing amplitudes) [17]. Second, the  $S$  matrix of the right-hand side of a  $\mathcal{PT}$  structure is  $\mathcal{P}S(n^*k)$ ,

so the right half of the  $\mathcal{PT}$  structure must have a resonance for waves incident from the left side as well, if its left side does. Therefore, the composite structure will have an ATR if either half does ( $r_{L,U} = 0$  or  $r_{R,V} = 0$ ). This argument is illustrated graphically in Fig. 4; we refer to these as trivial ATRs.

ATRs also occur when  $\text{Arg}[r_{L,U}]$  or  $\text{Arg}[r_{R,V}]$  equal  $(\alpha_U + \alpha_V)/2$  and involve multiple scattering between the subunits. It is straightforward to check that at such points,  $T = 1$  and  $R_L(R_R) = 0$ . It can be shown that a single layer of gain or loss in a lossless environment (e.g., in air) does not have transmission resonances in general, and we show in the Appendix that all the ATRs in Fig. 2 are of this type and are thus “nontrivial.”

As already noted, for an ATR to be bidirectional, a doubly accidental degeneracy is needed either in the amplitude of  $r_{L,U}$  and  $r_{R,V}$  ( $r_{L,U} = r_{R,V} = 0$ ) or their phase ( $\text{Arg}[r_{L,U}] = \text{Arg}[r_{R,V}] = (\alpha_U + \alpha_V)/2$ ). This is highly unlikely, unless one

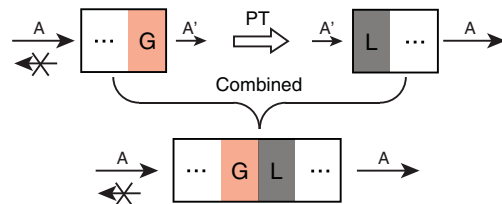


FIG. 4. (Color online) Graphical explanation of a trivial ATR arising from the transmission resonance of the left half in the right direction.  $\mathcal{PT}$  symmetry requires that it also be a resonance of the right half for left incidence (see argument in text). Depending on the particular  $\mathcal{PT}$  structure, there may or may not be trivial ATRs; for example, the simple heterostructure of Fig. 2(a) has no such ATRs. The ATRs of primary interest are those that arise from multiple scattering between the left and right halves of the structure.

can tune an additional continuous parameter other than the frequency, so in the generic case all transmission resonances of  $\mathcal{PT}$  structures are unidirectional.

In a recent work, Lin *et al.* [19] have studied a 1D  $\mathcal{PT}$ -symmetric Bragg structure of alternating dielectric layers with appropriate gain and loss, and discovered a series of very closely spaced ATRs centered around the Bragg point, with an additional property that they refer to as “unidirectional invisibility.” Not only do they find  $T = 1, R_L = 0, R_R \neq 0$  (or vice versa), as dictated by Eq. (9), they also find that at these ATRs, the transmission phase  $\phi_t = 0$ , corresponding to zero phase delay of the signal compared to free propagation. The properties of the ATRs also hold approximately in the neighboring frequency window, leading to a seemingly “broadband ATR.” For these reasons, there would be no signature of the presence of the structure in either the amplitude or phase of the received wave packet, if the wave is sent from the correct side (there would be a signature of course in the reflected wave if sent from the wrong side). This condition, that  $\phi_t = 0$  at the ATRs, is not required by our generalized unitarity relations and is specific to their structure [24]. A similar Bragg structure was studied before [25] and, recently, the equivalent Hermitian problem in a complex coordinate system was analyzed [26]. The “unidirectional invisibility” was shown to break down as the number of unit cells increases at a fixed modulation depth of the periodic refractive index [27], but a number of ATRs still exist in the vicinity of the Bragg point.

The existence of nontrivial ATRs is independent of whether the  $S$  matrix is in the  $\mathcal{PT}$ -symmetric or  $\mathcal{PT}$ -broken phase [13]; they can even occur at the symmetry-breaking exceptional point (see the following section). However, we do find for the simple gain-loss heterostructure of Figs. 2(a) and 2(b) that the ATRs disappear soon after the lasing threshold is passed in the broken-symmetry phase since in the large  $\text{Im}[n]kL$  limit,  $R_L R_R$  approaches unity asymptotically. This is not the case for more complicated  $\mathcal{PT}$  structures such as those of Fig. 2(c). The different behaviors of the two cases are illustrated in Fig. 10 of the Appendix and their origin is discussed.

#### IV. PHASE TRANSITION BOUNDARIES

A 1D  $\mathcal{PT}$  heterostructure can undergo a spontaneous symmetry-breaking transition in the eigenvalues and eigenvectors of its  $S$  matrix, as either  $\omega$  is increased at fixed gain or loss or as gain or loss is increased at fixed  $\omega$  [13]. In the symmetric phase, the  $\mathcal{PT}$  operation maps each scattering eigenstate back to itself, whereas in the broken-symmetry phase, each scattering eigenstate is mapped to the other. At the symmetry-breaking exceptional point, there is only one eigenvector and so both cases coincide.

Let  $\lambda_{1,2}$  be the eigenvalues of the  $S$  matrix of a  $\mathcal{PT}$ -symmetric heterostructure and  $v_{1,2}$  be the ratios of the two amplitudes of the corresponding eigenstates. It follows from the  $S$ -matrix parametrization (7) that

$$\lambda_{1,2} = \frac{i}{2a} [(b+c) \pm \sqrt{(b-c)^2 - 4}], \quad (15)$$

$$v_{1,2} = \frac{i}{2} [(c-b) \pm \sqrt{(b-c)^2 - 4}]. \quad (16)$$

These equations imply that  $\lambda_1 \lambda_2 = -|a|^2/a^2, v_1 v_2 = -1$ , and the eigenvalues must have reciprocal moduli. In the symmetric phase, both eigenvalues are unimodular, whereas the broken-symmetry phase corresponds to the  $|\lambda_1| > 1, |\lambda_2| < 1$  case. The exceptional point occurs when  $b - c = \pm 2$ , and there is a single eigenvector with eigenvalue  $\lambda = \pm i|a|/a$ . Both the eigenvalues and amplitudes  $v_{1,2}$  meet and bifurcate at the exceptional point, similar to the  $\mathcal{PT}$ -breaking transitions, which occur in the eigenvalue spectra of  $\mathcal{PT}$ -symmetric Hamiltonians [1–5].

Each eigenvector of the  $S$  matrix corresponds to a particular choice of two coherent beams, simultaneously directed at each side of the heterostructure. The  $S$ -matrix transition can in principle be observed by tuning the complex input amplitudes, measuring the output amplitudes, and hence finding the scattering eigenvalues. One would actually need to do such “two-sided” interference experiments to detect the attenuating mode in the broken-symmetry phase, an interesting possibility that is currently being explored [23]. However, such experiments with two coherent input beams [17] are often inconvenient and difficult to perform. Therefore, it would be preferable to have a criterion for the transition based on separate single-beam measurements.

In Ref. [13], two such criteria were given for the phase boundaries in an arbitrary  $\mathcal{PT}$ -symmetric heterostructure; however, they both involve the relative phase of the reflection and transmission coefficients. One of these conditions is  $r_L - r_R = \pm 2it$ . Using the conservation relations (9), this can be shown to lead to the simpler condition [28]

$$\frac{R_L + R_R}{2} - T = 1, \quad (17)$$

which involves only the transmittance and reflectances. The left-hand side of Eq. (17) is greater than unity in the broken-symmetry phase and less than unity in the  $\mathcal{PT}$ -symmetric phase. This provides a simple experimental criterion for locating the  $\mathcal{PT}$ -breaking transition point in 1D heterostructures. This criterion will be particularly useful if the quantity  $(R_L + R_R)/2 - T$  varies rapidly near the transition point. This appears to be the case for many heterostructures, as shown for example in Fig. 5 for a three-layer structure.

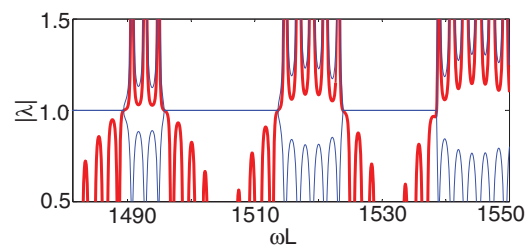


FIG. 5. (Color online) Test of the criterion (17) for  $\mathcal{PT}$ -symmetry-breaking points of a three-layer heterojunction structure. The thin solid lines represent the eigenvalues of the  $S$  matrix, which exhibit five symmetry-breaking points as the frequency  $\omega$  is tuned over the selected range. The thick solid line indicates the left-hand side of Eq. (17). The heterostructure has a constant  $\text{Re}[n] = 3$ , and the first and last layers are filled with gain and loss of  $\text{Im}[n] = \pm 0.005$ . The width of the central passive region is 4% of the total length  $L$ .

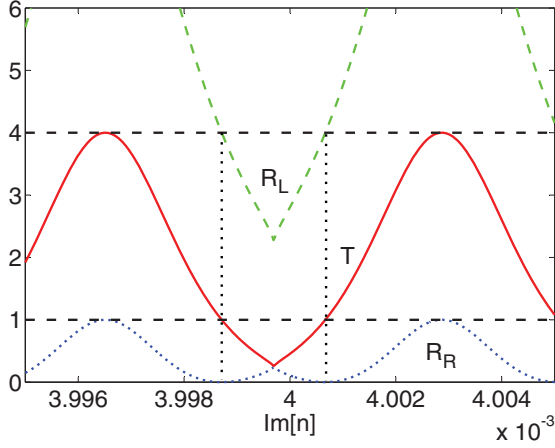


FIG. 6. (Color online) Reflectances and transmittance along the  $\mathcal{PT}$  phase boundary for the 1D  $\mathcal{PT}$ -symmetric structure studied in Fig. 2(a), in the high-frequency regime ( $\omega L \gtrsim 1725$ ). The plots are given as a function of the gain or loss strength  $\text{Im}[n]$ , while the frequency  $\omega$  is simultaneously varied to maintain the system at the phase boundary. Vertical dotted lines indicate points where  $R_R = 0$ , for which  $R_L = 4$  and  $T = 1$  as predicted by Eq. (17) and indicated by horizontal dashed lines.

Equation (17) implies that for an ATR to coincide with the exceptional point, the nonzero reflectance must be exactly equal to 4, which is allowed but will not occur without specific tuning. An example of such tuning is shown in Fig. 6. This plot is obtained by tuning both the gain or loss strength ( $\text{Im}[n]$ ) and the frequency, to keep the system along the phase boundary, and observing the reflectances and transmittance. Two ATRs are found along the phase boundary. We note that a special set of solutions of Eqs. (9) and (17) are given by  $R_R, R_L, T = (p \pm 1)^2, p^2, (p \mp 1)^2$ , where  $p$  is an arbitrary real number. Interestingly, the maxima of  $R_R, R_L, T$  in this simple geometry are given by this set of solutions with  $p = \text{Re}[n]$  in the high-frequency regime where  $\text{Im}[n] \ll 1$ .

## V. UNIQUENESS OF $\mathcal{PT}$ TRANSITION IN SCATTERING

The generalized unitarity relations (8)–(10) hold regardless of whether the eigenvalues and eigenvectors of the  $S$  matrix are in the  $\mathcal{PT}$ -symmetric or  $\mathcal{PT}$ -broken phase, although the quantities in the generalized unitarity relations are related to the phase of the  $\mathcal{PT}$  scattering system through the relation (17). There is, however, some freedom of choice in the definition of the 1D  $S$  matrix, corresponding to permutation of the outgoing channels. The definition we used in Ref. [13] is given in Eq. (6), which is also widely used in mesoscopic physics [29]. In this section, we will refer to the  $S$  matrix defined in this way as  $S_0$ . In  $S_0$ , the reflection coefficients are on the diagonal, and the outgoing channels are related to the corresponding incident channels by time reversal, which seems quite natural. In particular, the time-reversal operation  $\mathcal{T}$  in this definition is represented by the complex conjugation operator.

There is, however, an alternate definition:

$$\begin{pmatrix} D \\ A \end{pmatrix} = S_c \begin{pmatrix} B \\ C \end{pmatrix} \equiv \begin{pmatrix} t & r_L \\ r_R & t \end{pmatrix} \begin{pmatrix} B \\ C \end{pmatrix}, \quad (18)$$

which has also been used in the literature, including in one of the earliest works on  $\mathcal{PT}$ -symmetric scattering by Cannata *et al.* [30]. This alternative definition of the  $S$  matrix, which we will refer to as  $S_c$ , was subsequently used in the work on unidirectional invisibility of Lin *et al.* [19]. Because the permutation operation does not preserve the eigenvalues, these two different definitions of the  $S$  matrix lead to different criteria for the symmetric and broken-symmetry phases, as well as for the phase boundary (exceptional points). This can lead to confusion, as well as raising questions as to whether the  $S$ -matrix eigenvalues and eigenvectors, and their transitions, are physically meaningful.

Note first that both definitions lead to the same values for  $t, r_R, r_L$ , so they will give the same scattered state for the same input state. The issue is whether one or the other definition more closely reflects the phenomena of spontaneous  $\mathcal{PT}$ -symmetry breaking, as already known from Hamiltonian studies. In our earlier work on the  $\mathcal{PT}$  transition in scattering systems [13], we showed that the phase boundary of  $S_0$  corresponds closely to the anticrossings of the poles of the  $S$  matrix in the complex  $\omega$  plane (see also [15]). The locations of these poles are independent of the definition of  $S$ ; they reflect the internal excitation frequencies of the scatterer, as well as the coupling of these excitations to the continuum. This suggested that the  $\mathcal{PT}$  transition of  $S_0$  is indeed associated with the  $\mathcal{PT}$  transition of some underlying effective  $\mathcal{PT}$ -symmetric Hamiltonian. We have recently verified this point of view analytically and numerically, in collaboration with others. The main part of that work will be presented elsewhere [31]; here, we just state a few relevant results and show a numerical example corroborating this point of view.

First, it is straightforward to show that the eigenvalues of  $S_c$  have the same general properties as those of  $S_0$  (even though they do not coincide). In particular, their product is  $-1$  and they are either both unimodular or of reciprocal modulus. However, the criterion for their exceptional points differs from that of  $S_0$ . Using a similar  $a, b, c$  parametrization of  $S_c$  as used earlier for  $S_0$ , one finds that the eigenvalues are given by

$$\lambda_1, \lambda_2 = \frac{1}{a} [1 \pm \sqrt{-bc}]. \quad (19)$$

Since both  $b$  and  $c$  are real, this expression shows that when  $bc > 0$  both eigenvalues are complex (and unimodular), whereas when  $bc < 0$ , both eigenvalues are real and satisfy  $|\lambda_1| = |\lambda_2|^{-1} \neq 1$ . Exceptional points occur when  $b = 0$  or  $c = 0$ . From Eqs. (7) and (8), one sees that  $bc = (1/T - 1)$  and so  $bc > 0 \rightarrow T < 1$  and  $bc < 0 \rightarrow T > 1$ , while  $b = 0 (r_L = 0)$  or  $c = 0 (r_R = 0)$  is the condition for  $T = 1$ . Thus, each ATR is an exceptional point for  $S_c$ , and  $T > 1$  corresponds to the “broken-symmetry” phase, whereas  $T < 1$  to the “symmetric” phase. This is in contrast to  $S_0$  for which one has the criterion of Eq. (17) involving both  $T$  and the average of  $R_L$  and  $R_R$ .

These two conditions for the transition and for the two phases of the  $S$  matrix do not coincide [see Figs. 7 and 8(a)] unless an ATR is tuned to occur at the phase boundary of  $S_0$  as we have shown in Fig. 6. We see that for this simple heterostructure,  $S_0$  has a single transition to the broken-symmetry phase (for a fixed  $\text{Im}[n]$ ), while  $S_c$  has a series of transitions corresponding to entering and leaving the broken-symmetry phase in the high-frequency regime (Fig. 7). Each

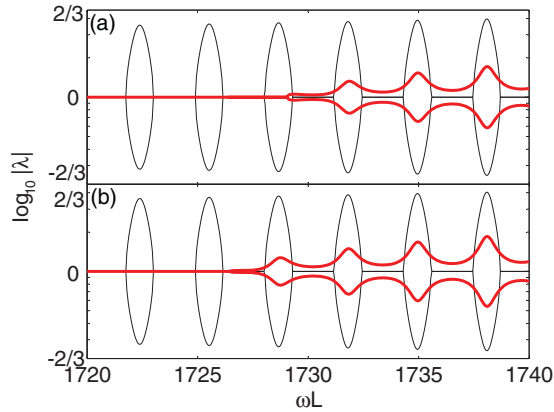


FIG. 7. (Color online) Logarithm of the modulus of the eigenvalues of  $S_0$  (thick line) and  $S_c$  (thin line) for the 1D  $\mathcal{PT}$  heterostructure studied in Fig. 2(a); case (a) is with  $\text{Im}[n] = 3.995 \times 10^{-3}$  and case (b) is with  $\text{Im}[n] = 4 \times 10^{-3}$ .  $|\lambda| = 1$  indicates the  $\mathcal{PT}$ -symmetric phase, and reciprocal values for  $|\lambda|$  indicate the broken-symmetry phase.  $S_c$  has multiple “transitions” spaced by the free spectral range and insensitive to  $\text{Im}[n]$ ;  $S_0$  has a single transition, which is highly sensitive to small changes in  $\text{Im}[n]$ .

of these transitions begins at one of the two ATRs and ends at the other; thus, the centers of the broken-symmetry regions are spaced by the free spectral range of the unitary cavity. These “lozenges” of broken-symmetry phase barely change when  $\text{Im}[n]$  is varied;  $S_c$  repeatedly enters and leaves the symmetric phase as we tune  $\omega$ . In contrast, the single transition point of  $S_0$  moves substantially to lower frequency as  $\text{Im}[n]$  increases; once it enters the broken-symmetry phase, it never reenters the symmetric phase at any higher frequency. This indicates that  $S_0$ , not  $S_c$ , is measuring the breaking of  $\mathcal{PT}$  symmetry.

In Fig. 8, we show the decisive comparison. If we simply take the  $\mathcal{PT}$  heterostructure shown in Fig. 2(a), and impose Dirichlet or Neumann boundary conditions at the boundaries to the continuum, we have a non-Hermitian discrete eigenvalue problem with  $\mathcal{PT}$  symmetry. Its energy spectrum (expressed as complex frequencies) makes transitions between real and complex conjugate pairs [Fig. 8(b)] in a manner that perfectly follows the behavior of the eigenvalues of  $S_0$  and but not of  $S_c$  [Fig. 8(a)]. Moreover, in Fig. 8(c) we show the poles and zeros of the  $S$  matrix; their symmetric distribution around the  $\text{Im}[k]$  axis is a consequence of the  $\mathcal{PT}$  symmetry. Before the  $\mathcal{PT}$  transition of  $S_0$ , the poles have approximately the same value of  $\text{Im}[k]$  as for the passive system, but just at the transition of  $S_0$ , there is an anticrossing in the complex plane and half begin moving toward the real axis and the other half recede further down in the complex plane [13, 15]. For  $\text{Im}[k] \approx 17$ , the system is very near the CPA laser point for which a pole and zero coincide on the real axis. The eigenvalues of both  $S_0$  and  $S_c$  diverge or vanish at this point because  $t$ ,  $r_R$ , and  $r_L$  all diverge at the lasing transition. Interestingly, for this value of  $\text{Im}[n]$ , there are no ATRs after the lasing transition and  $T < 1$  for all larger  $k$ ; the reasons for this are discussed in the Appendix. The same correspondence between the broken-symmetry phase of  $S_c$  and the analogous closed-system Hamiltonian holds for more complex  $\mathcal{PT}$  heterostructures, such as that of Fig. 2(c), where  $S_0$  has multiple broken phases [31]. Thus, we believe that at

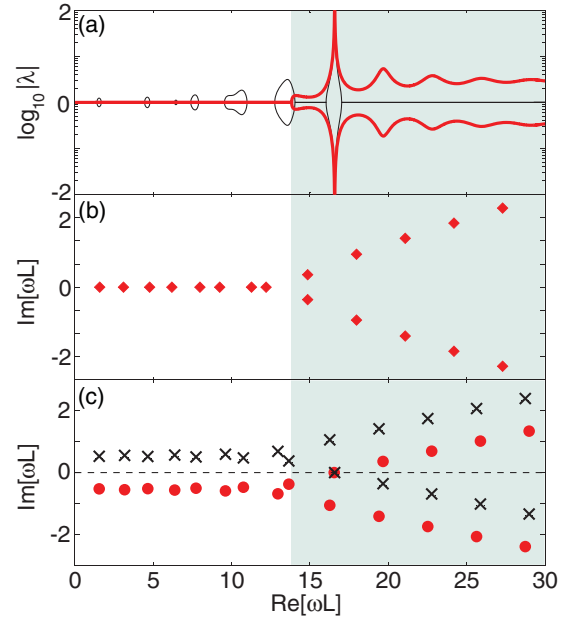


FIG. 8. (Color online) (a)  $\mathcal{PT}$  phase transition of  $S_0$  (thick line) and  $S_c$  (thin line) for the 1D heterostructure studied in Fig. 2(a) but with  $n = 2 \pm 0.208i$ . The broken-symmetry phase of  $S_0$  is indicated by the shadowed area. (b)  $\mathcal{PT}$  phase transition of the corresponding finite non-Hermitian cavity Hamiltonian with Dirichlet boundary conditions. Its broken-symmetry phase coincides with that of  $S_0$ . (c) Poles (red circles) and zeros (black crosses) of the  $S$  matrix (which are the same for  $S_0$  and  $S_c$ ); anticrossing of the poles occurs at the phase transition of  $S_0$ . At  $kL \approx 17$ , the system is very near the CPA laser threshold point, where the cavity both emits laser radiation and perfectly absorbs the time reversal of the lasing mode.

least for the 1D case, there is a unique definition of the  $S$  matrix, under which its  $\mathcal{PT}$  transitions actually reflect the symmetry breaking in the underlying non-Hermitian Hamiltonian.

## VI. CONCLUSION

We have derived generalized unitarity relations for the  $S$  matrix of arbitrary 1D  $\mathcal{PT}$ -symmetric photonic heterostructures, including a conservation relation between the transmittance and the left and right reflectances. This conservation relation can be easily tested in experimental structures and used as a criterion of how precisely one has realized the  $\mathcal{PT}$  symmetry. In addition, the conservation relation leads to a simple criterion for identifying the exceptional point(s) at which the  $\mathcal{PT}$  symmetry is spontaneously broken or restored. These exceptional points are shown to be closely related to the  $\mathcal{PT}$ -symmetry-breaking transition of the underlying effective Hamiltonian of the system.

## ACKNOWLEDGMENTS

We thank T. Kottos, S. Rotter, K. Makris, H. Ramezani, Z. Lin, H. Cao, D. Christodoulides, and C. West for helpful conversations. This work was supported by NSF Grant No. ECCS 1068642.

### APPENDIX: PROPERTIES OF SIMPLE GAIN-LOSS HETEROJUNCTION

The  $\mathcal{PT}$  heterostructure shown in Fig. 2(a), which consists of two uniform slabs of equal length and index  $n, n^*$ , is the simplest example one can study of the class of 1D  $\mathcal{PT}$ -symmetric photonic heterostructures, and it has been treated previously in [11,13]. We will refer to this structure as the “simple heterojunction” (SH), and it is described by the transfer matrix (4) with  $a = (\alpha + \alpha^*) + i(\beta + \gamma)$ ,  $b = -i(\alpha - \alpha^*) + (\gamma - \beta)$ , and  $c = i(\alpha - \alpha^*) + (\gamma - \beta)$ , where

$$\alpha = \frac{|\cos \Delta|^2}{2} - \frac{n^*}{2n} |\sin \Delta|^2, \quad (\text{A1})$$

$$\beta = \frac{1}{2|n|^2} [n^* \sin \Delta \cos \Delta^* + \text{c.c.}], \quad (\text{A2})$$

$$\gamma = \frac{1}{2} [n \sin \Delta \cos \Delta^* + \text{c.c.}], \quad (\text{A3})$$

and  $\Delta \equiv nkL/2$  is the complex optical path inside the left half. Since  $\beta, \gamma$  are real, so are  $b$  and  $c$ , and it is straightforward to check that (5) holds. This transfer matrix leads to certain simple properties. First, as mentioned in the text, the SH has no trivial ATRs as we will show in Sec. 1. Second, below the  $\mathcal{PT}$ -symmetry-breaking point, it has many ATRs, roughly two per free spectral range of the passive resonator. Above the symmetry-breaking transition, it still has ATRs until it passes the lasing transition after which they disappear in the limit  $\text{Im}[nkL] \rightarrow \infty$ . We will discuss this behavior and contrast it with more complex heterostructures in Sec. 2.

#### 1. Absence of trivial ATRs

The SH can be treated as having an air gap of vanishing width in-between the gain and loss regions. Hence, the absence of trivial ATRs is a consequence of the absence of reflectionless transmission resonances of such uniform amplifying or attenuating slabs in air. In the following, we first discuss in general the transmission resonances of a uniform slab of refractive index  $n$  and length  $L/2$  embedded in two semi-infinite media of index  $n_l$  and  $n_r$ .

For this simple setup, the transfer matrix defined in Sec. II [( $\begin{smallmatrix} A \\ B \end{smallmatrix}$ ) =  $M(\begin{smallmatrix} C \\ D \end{smallmatrix}$ ); see Fig. 1] takes the form

$$M = \frac{1}{2} \begin{pmatrix} 1 & \frac{1}{n_l k} \\ 1 & -\frac{1}{n_l k} \end{pmatrix} \begin{pmatrix} \cos \Delta & i \frac{\sin \Delta}{nk} \\ ink \sin \Delta & \cos \Delta \end{pmatrix} \begin{pmatrix} 1 & 1 \\ n_r k & -n_r k \end{pmatrix}, \quad (\text{A4})$$

where  $n_l, n_r, n$  can be complex. A transmission resonance of an incident beam from the left side requires  $C = 0$  and

$$A = \left(1 - \frac{n_r}{n_l}\right) \cos \Delta + i \left(\frac{n}{n_l} - \frac{n_r}{n}\right) \sin \Delta = 0. \quad (\text{A5})$$

For the gain and loss regions in SH, when treated as being separated by an infinitely thin air gap,  $n_l = n_r = 1$  while  $\text{Im}[n] \equiv \tau \neq 0$ . We immediately see that Eq. (A5) can not be satisfied because  $\sin \Delta \neq 0$  due to the finite imaginary part of  $n$ . This holds independent of  $n$  ( $\tau \neq 0$ ) and  $k$  ( $\neq 0$ ) (see Fig. 9). This finding is confirmed by calculating the reflectance directly [see Fig. 9(a)]. The same analysis can be extended to the slightly more complicated case shown in Fig. 2(c), where

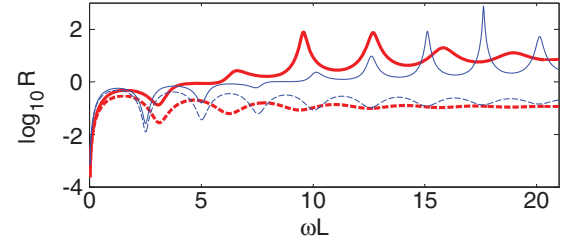


FIG. 9. (Color online) Reflectance of the gain (solid) and loss (dashed) region in the heterostructure studied in Fig. 2(a). Two values of the refractive index are considered:  $n = 2 \pm 0.2i$  (thick),  $n = 2.5 \pm 0.1i$  (thin).

all the ATRs are also found to be “nontrivial” as confirmed again by calculating the reflectances of the subunits directly. We note, however, that trivial ATRs do exist in some  $\mathcal{PT}$  structures. An example is the concatenation of even numbers of SHs.

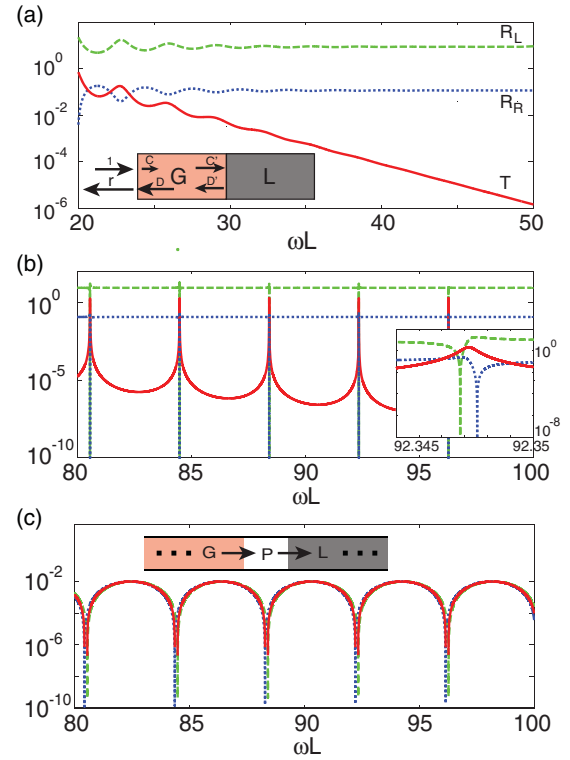


FIG. 10. (Color online) (a) Reflectances and transmittance same as in Fig. 2(a) but at higher frequencies. Inset: Analysis of the reflection coefficient from the “gain” side. Letters with arrow represent the complex amplitude of the traveling waves at the nearest interface. (b) Reflectances and transmittance same as in Fig. 2(c), but at higher frequencies. Inset: zoomed in on the two ATRs near  $\omega L = 92.35$ . (c) Reflectances and transmittance of the central passive region in Fig. 2(c) placed between two semi-infinite regions of gain and loss with  $n = 2 \pm 0.2i$ . The transmission resonances are given by Eq. (A6) in which  $\text{Im}[n_l]$  takes opposite signs depending on the propagation direction. Solid curve represents  $T - 1$  and its broken parts indicate  $T < 1$ .



**2. Asymptotic properties of ATRs in the simple heterojunction**

In this main text, we noted that ATRs for the SH disappear soon after the lasing threshold is passed in the broken-symmetry phase of  $S_0$  [see Fig. 10(a)]. To understand this observation, we study the behaviors of  $R_R$  and  $R_T$  in the large  $\tau kL$  limit. The reflection coefficient from the “loss” side of the  $\mathcal{PT}$  heterostructure approaches the value given by the Fresnel formula  $(1 - n)/(1 + n)$  due to the suppression of interference effects by strong absorption. Surprisingly, the asymptotic value of the reflection coefficient from the “gain” side,  $(1 + n^*)/(1 - n^*)$ , turns out to be the inverse of the Fresnel formula. This can be explained from the analysis shown by the inset of Fig. 10(a). Due to the strong loss inside the “loss” side of the cavity,  $D'$  is given by the Fresnel relation  $C'(2n^*)/(n^* - n) \equiv C'r'$ , implying  $|D| = |\exp[in^*kL/2]D'| = |r' \exp[in^*kL]C|$  is much larger than  $|C|$  in the large  $\tau kL$  limit. Therefore, the scattering at the air-gain interface is approximately the time-reversed process as if the “gain” side (which is the “loss” side in the time-reversed picture) were semi-infinite, i.e., with incident amplitude  $r^*$  and reflected amplitude 1 in the air and transmitted amplitude  $D^*$ , satisfying the Fresnel relation. The reflection coefficient in the original problem is then  $(1 + n^*)/(1 - n^*)$ . Thus,  $R_L R_R \rightarrow 1$  in this limit, which implies  $T \rightarrow 0$  from Eq. (9) and ATRs do not exist.

In more complicated  $\mathcal{PT}$  structures, ATRs can take place in this limit. For example, the reflection coefficient connecting  $C'$  and  $D'$  approaches zero at the transmission resonances of the passive region in Fig. 2(c). The analysis above then breaks down and sharp changes of the transmittance and reflectances take place at these frequencies as shown in Fig. 10(b). These transmission resonances through the passive region are a special set of solutions of Eq. (A5). They require  $n_l = n_r^*$  and  $\text{Im}[n] = 0$ , and the transmission resonances occur at

$$\Delta = \arctan \left[ \frac{2 \text{Im}[n_l]n}{\text{Re}[n_l]^2 - \text{Im}[n_l]^2 - n^2} \right]. \quad (\text{A6})$$

In the frequency range shown in Fig. 2(c) where  $\text{Im}[n_l]k$  is small, these transmission resonances do not lead to ATRs of the whole heterostructure due to the multiple interferences taking place inside the gain and loss sub-units. In the large  $\text{Im}[n_l]k$  limit shown in Fig. 10(b), however, these multiple interferences are suppressed due to strong absorption or amplification, and ATRs arise from the resonances given by (A6). Note that these ATRs are still “nontrivial” as the frequencies given by (A6) are not the transmission resonances of the gain or loss subunit in the absence of the other.

For the purpose of completeness, we mention a few more cases where transmission resonances of a single uniform slab [i.e., the solutions of Eq. (A5)] exist. When  $n_l, n_r, n$  can be treated as real (with negligible absorption and no gain), two types of solutions of (A5) can be found. The first one is well known,  $n_l = n_r$ , which requires  $\sin \Delta = 0$ ; the second one is less well known,  $n = \sqrt{n_l n_r}$ , which requires  $\cos \Delta = 0$ . It is easy to convince oneself that no other types of solution exist for real indices. As one slowly increases the gain or loss strength in the scattering layer, approximate transmission resonances can still be found, but their reflectances gradually increase and eventually become detectable. In Ref. [32], a different case was studied where  $n_r = 1$ ,  $\text{Im}[n] = 0$ ,  $\text{Im}[n_l] \neq 0$ . By noticing that  $\cos \Delta = 0$  can not satisfy the above equation and  $\tan \Delta$  is real, Eq. (A5) can be reduced to

$$\text{Im}[n_l]^2 = (\text{Re}[n_l] - 1)(n^2 - \text{Re}[n_l]), \quad (\text{A7})$$

$$\tan \Delta = -n \left( \frac{\text{Re}[n_l] - 1}{n^2 - \text{Re}[n_l]} \right)^{\frac{1}{2}}. \quad (\text{A8})$$

It describes the transmission resonance from a loss or gain media to air through a passive slab, which gives rise to the novel “surface” lasing modes introduced in Ref. [32].

---

[1] C. M. Bender and S. Boettcher, *Phys. Rev. Lett.* **80**, 5243 (1998).  
 [2] C. M. Bender, S. Boettcher, and P. N. Meisinger, *J. Math. Phys.* **40**, 2201 (1999).  
 [3] C. M. Bender, D. C. Brody, and H. F. Jones, *Phys. Rev. Lett.* **89**, 270401 (2002).  
 [4] R. El-Ganainy, K. G. Makris, D. N. Christodoulides, and Z. H. Musslimani, *Opt. Lett.* **32**, 2632 (2007).  
 [5] K. G. Makris, R. El-Ganainy, D. N. Christodoulides, and Z. H. Musslimani, *Phys. Rev. Lett.* **100**, 103904 (2008).  
 [6] C. E. Rüter, K. G. Makris, R. El-Ganainy, D. N. Christodoulides, M. Segev, and D. Kip, *Nat. Phys.* **6**, 192 (2010).  
 [7] M. C. Zheng, D. N. Christodoulides, R. Fleischmann, and T. Kottos, *Phys. Rev. A* **82**, 010103(R) (2010).  
 [8] A. Guo, G. J. Salamo, D. Duchesne, R. Morandotti, M. Volatier-Ravat, V. Aimez, G. A. Siviloglou, and D. N. Christodoulides, *Phys. Rev. Lett.* **103**, 093902 (2009).  
 [9] Z. H. Musslimani, K. G. Makris, R. El-Ganainy, and D. N. Christodoulides, *Phys. Rev. Lett.* **100**, 030402 (2008).  
 [10] H. Ramezani, T. Kottos, R. El-Ganainy, and D. N. Christodoulides, *Phys. Rev. A* **82**, 043803 (2010).  
 [11] A. Mostafazadeh, *Phys. Rev. Lett.* **102**, 220402 (2009).  
 [12] S. Longhi, *Phys. Rev. A* **82**, 031801(R) (2010).  
 [13] Y. D. Chong, Li Ge, and A. D. Stone, *Phys. Rev. Lett.* **106**, 093902 (2011).  
 [14] H. Schomerus, *Phys. Rev. Lett.* **104**, 233601 (2010).  
 [15] Gwangsuo Yoo, H.-S. Sim, and H. Schomerus, *Phys. Rev. A* **84**, 063833 (2011).  
 [16] Y. D. Chong, Li Ge, H. Cao, and A. D. Stone, *Phys. Rev. Lett.* **105**, 053901 (2010).  
 [17] W. Wan, Y. D. Chong, L. Ge, H. Noh, A. D. Stone, and H. Cao, *Science* **331**, 889 (2011).  
 [18] A. Mostafazadeh, *J. Math. Phys.* **45**, 932 (2004).  
 [19] Z. Lin, H. Ramezani, T. Eichelkraut, T. Kottos, H. Cao, and D. N. Christodoulides, *Phys. Rev. Lett.* **106**, 213901 (2011).  
 [20] Here, we assume the refractive indices  $n_l, n_r$  on the left and right sides of the 1D structure are the same. A more general relation is

- $\det(M) = n_l/nr$ ; see A. Yeh, *Optical Waves in Layered Media* (Wiley, New York, 1988).
- [21] When  $M_{11}, M_{22} = 0$ , the two incident amplitudes  $B, C$  and the two outgoing amplitudes  $A, D$  become decoupled, which gives rise to the CPA laser points and the reflection and transmission coefficients become infinite. However, the results derived in the main text are still valid at these points with appropriate choices of limiting procedures.
- [22] S. Longhi, *Phys. Rev. Lett.* **107**, 033901 (2011).
- [23] A. D. Stone *et al.* (unpublished).
- [24] There may seem to be a number of frequencies in Fig. 2(b) at which  $T = 1$  and  $\phi_r \approx 0$ , but it is a coincidence as the transmission phase oscillates around  $nkL$  and we have chosen  $\text{Re}[n]$  to be an integer.
- [25] M. Kulishov, J. Laniel, N. Bélanger, J. Azaña, and D. Plant, *Opt. Express* **8**, 3068 (2005).
- [26] H. F. Jones, *J. Phys. A: Math. Theor.* **44**, 345302 (2011).
- [27] S. Longhi, *J. Phys. A: Math. Theor.* **44**, 485302 (2011).
- [28] Alternatives include  $\sqrt{R_L} = 1 \pm \sqrt{T}$  and  $\sqrt{R_R} = 1 \mp \sqrt{T}$ , but they suffer from a sign uncertainty, an artifact different from the two physical possibilities in  $r_L - r_R = \pm 2it$ .
- [29] C. W. J. Beenakker, *Rev. Mod. Phys.* **69**, 731 (1997).
- [30] F. Cannata, J. P. Dedonder, and A. Ventura, *Ann. Phys. (NY)* **322**, 397 (2007).
- [31] S. Rotter *et al.* (unpublished).
- [32] Li Ge, Y. D. Chong, S. Rotter, H. E. Türeci, and A. D. Stone, *Phys. Rev. A* **84**, 023820 (2011).